Radar Cross-Section Modeling of Marine Vessels in Practical Oceanic Environments for High-Frequency Surface-Wave Radar

Symon K. Podilchak [1], Hank Leong [2], Ryan Solomon [1], Yahia M. M. Antar [1]

[1]*Electrical and Computer Engineering, Royal Military College of Canada*
Kingston, Ontario, Canada (email: antar-y@rmc.ca)
[2]*Defence R&D Canada (DRDC)*
Ottawa, Ontario, Canada (email: hank.leong@drdc-rddc.gc.ca)

***Abstract*— Models of the Teleost marine vessel and the Bonn Express cargo freighter are developed for generation of monostatic and bistatic radar cross section (RCS) returns for high-frequency surface-wave radar (HFSWR). Simulated monostatic RCS values are in good agreement with measured values at 4.1 MHz, thus additional investigations, to model varied practical situations may also be of interest. Specifically, the effects of pitch and roll and ship displacement (due to cargo container loading) are studied. Results show that the monostatic RCS of the Teleost can vary by more than 10 dB for a 10° roll or a 15° pitch incline. These results also suggest that the monostatic RCS of the Teleost has a null at broadside at the radar frequency of 7 MHz likely due to the resonant scattering of the A-frame mast and antenna structures. In addition, by modeling the Bonn Express with a full load and varied displacement, a very good agreement between the measured and simulated RCS can be observed.**

I. Introduction

High-frequency surface-wave radar (HFSWR) is a cost effective means for remote sensing and surveillance of marine vessels. In such radar systems, high-frequency (HF) vertically polarized energy is radiated from a transmit source, resulting in surface-waves (SWs) which hug the curvature of the earth along a sea surface. Long monostatic and bistatic radar ranges, in the order of hundreds of kilometres, can be achieved in such HF systems due to the low attenuation of the propagating SW along the conducting sea surface.

One difficulty in implementing such radar systems is accurate knowledge of the target, or more specifically, the radar cross-section (RCS) of the scatterer or vessel of interest. There is little information in the open literature regarding the RCS values of marine vessels in the HF band. An empirical formula developed in [1] for vessel RCS in the microwave frequency range is sometimes used to approximate returns at HFs. However, this formula does not account for the vertical structures of the marine vessels which may be in resonance. Furthermore, inclusion of additional vessel characteristics, such as pitch and roll variations and ship displacement, can increase modeling complexity and be problematic for accurate RCS prediction.

In [2] and [3], commercially available software tools (NEC and FEKO) were used to model the RCS of different marine vessels. Specifically, monostatic return values were compared to the measured results from two ships: the Teloest (a 2405-ton Canadian Coast Guard vessel) and the Bonn Express (a 36000-ton cargo freighter). A good agreement was achieved when compared to measurements. This work extends the previous investigations by developing new FEKO models and including the effects of various practical situations that can occur in oceanic environments. Specifically, the effects of pitch and roll (due to unforeseen weather conditions) and the effects of ship loading (due to cargo containers) on RCS is examined. In addition, by modeling the Bonn Express cargo freighter with a full load and varied displacement, a very good agreement between the measured and simulated RCS is observed.

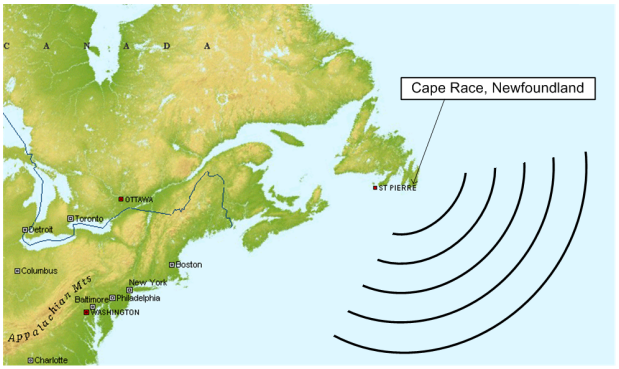

Fig. 1. An illustration of the HFSWR coverage area near Cape Race, Newfoundland, Canada. Measurements (completed in February 2002) offer a validation for numerical models that investigate pitch and role, loading effects and other practical situations in oceanic environments.

II. Radar Cross-Section Measurements and Analysis of Developed FEKO Models

Measurements of the Teleost and Bonn Express were completed in February, 2002 using the HFSWR system in Cape Race, Newfoundland, Canada (see Fig. 1). These two ships were modeled and their monostatic RCS values were originally computed in [2] and [3] using NEC and FEKO, respectfully. In this work, we use the base model in [3] for the Teleost to study the effects of pitch and roll on the RCS, and we develop

978-1-4244-2871-7/09/$25.00 ©2009 IEEE

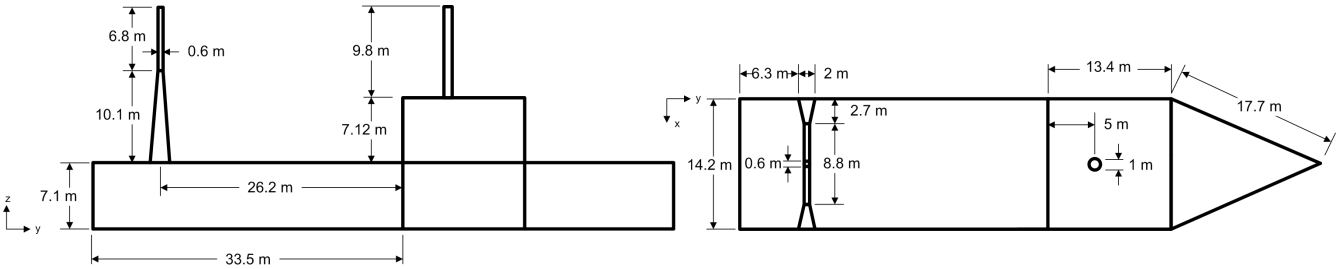

Fig. 2. Top view and side view (port or starboard) of the modeled Teleost vessel.

Fig. 3. Photograph of a Teleost vessel used in the Canadian Coast Guard. The length and breadth of the ship was 63 m and 14.2 m, respectively.

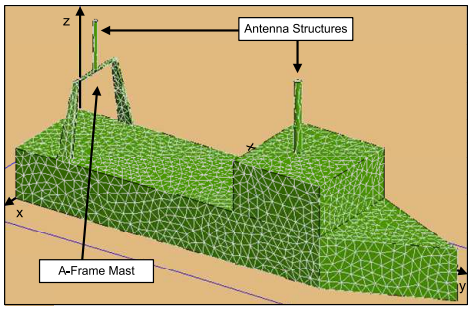

Fig. 4. Teleost base model with A-frame mast and antenna structures.

a new model for the Bonn Express to study the effects of ship displacement. Illustrations, characteristics and dimensions of the vessels and the FEKO models are shown in Figs. 2-8. All models utilized a perfectly electrical conducting (PEC) ground plane to represent the ocean surface. Comparison of these measured RCS returns to simulated values is crucial in model development, refinement and accuracy. In addition, the top view of a generic ship is shown in Fig. 5 to provide reference to vessel RCS at various aspects.

A. Radar-Cross Section Measurements and Developed Models

The Teleost vessel was used as a test target providing RCS measurements. Monostatic returns were acquired at every 30 degrees from the bow direction, including stern and broadside aspects. The radar was calibrated using first-order sea echoes (Bragg lines) measured under stormy sea conditions. The sea was assumed to be fully developed at that time, and therefore, the scattering coefficient derived by Barrick for the first-order sea echo [4] was used in the calibration. The results indicate that the RCS of the Teleost is 40.5 dBm^2 at 4.1 MHz for stern incidence. The Teleost was then modeled and the monostatic RCS was computed using NEC in [2] and FEKO in [3]. The computed RCS values agree well with the measurements as shown in Fig. 9.

Similarly, the Bonn Express was tracked outbound and measured returns were compared with the first-order sea echoes to calculate the monostatic RCS. While the computed RCS values in [2] and [3] mostly agreed with the measured values, there was always disagreement in one of the off broadside peaks. In this paper, we advance the base model of the Bonn Express in [3] by adding a cargo load, fore- and after-masts, adjusting the ship displacement due to loading, and by adding a small walking area around the ship (Fig. 8). With these inclusions, there is a very good agreement between the measured and simulated RCS as shown in Fig. 10.

B. Analysis of the Simulated Radar Cross-Section

Since a very good agreement between the measured and simulated RCS is observed at 4.1 MHz additional investigations, using similar methodologies, may also prove to be valid. It should be noted that the model of Teleost is the same as the one used in [3] while the model of the Bonn Express is advanced by modeling the fore- and after-masts, including ship displacement due to cargo loading and by

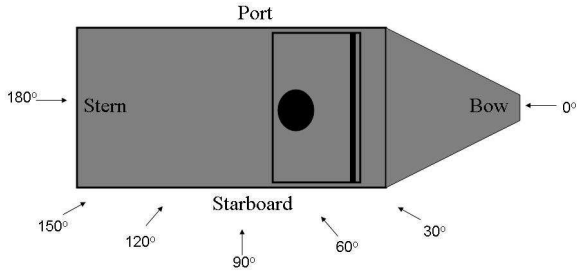

Fig. 5. Top view of a standard ship and angles of incident fields referenced to the port, starboard, bow and stern.

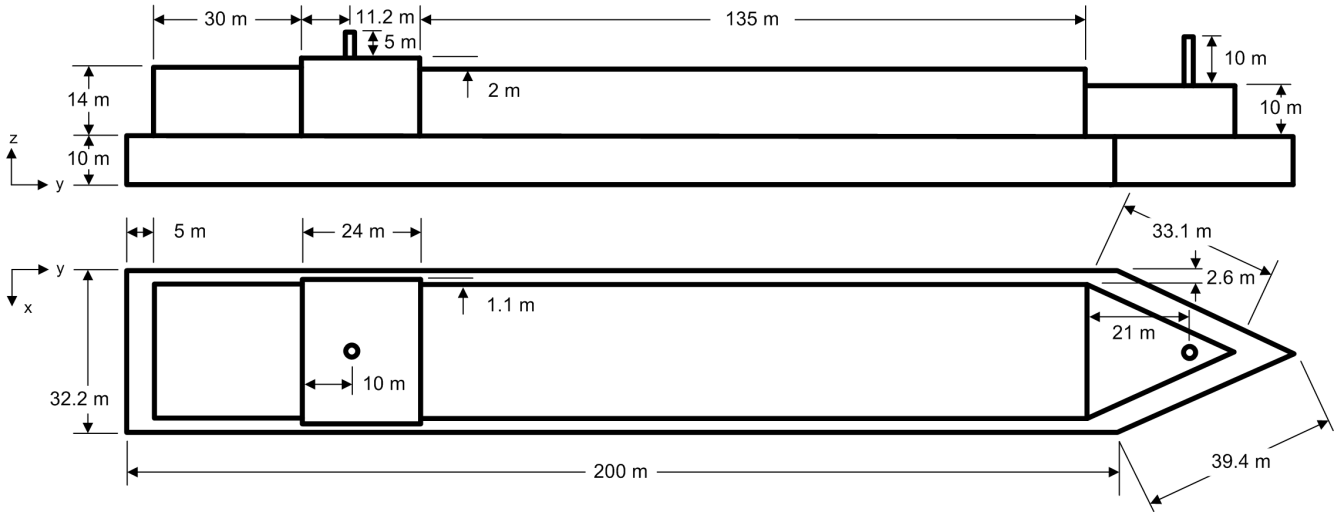

Fig. 6. Top view and side view (port or starboard) of the modeled Bonn Express freighter (antennae structure radii 1 m).

Fig. 7. Photograph of the Bonn Express cargo freighter. The multiple storage containers are illustrated. The Bonn Express had a length of 236 m and a width of 32 m [2].

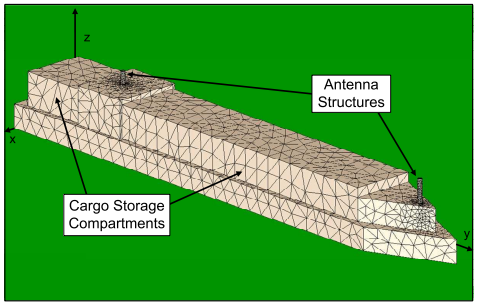

Fig. 8. Bonn Express model with cargo storage compartments and ship displacement due to loading.

adding a small walking area around the ship. With these inclusions, the model achieves a very good agreement with the measured and simulated RCS for the Bonn Express freighter. Furthermore, to illustrate the RCS as a function of frequency, additional simulations were completed for the two ships. Figs. 11 and 12 respectfully show the monostatic and bistatic (for broadside, $90°$, incidence) RCS of the Teleost from 1 to 20 MHz. Similarly, Fig. 13 shows the monostatic returns of the Bonn Express cargo freighter from 1 to 7 MHz.

It is interesting to note that for the Teleost a broadside null is observed in the RCS at 7 MHz as shown in Fig. 11. The antenna and A-frame structures may resemble resonant scatterers, which are generally of the order of one-half to 10 wavelengths in size [5] causing a destructive resonant scattering effect. For instance, at 7 MHz $\frac{\lambda_0}{2} = 21.4$ m. This half-wavelength distance is approximately equal to the height of the modeled A-frame mast and stern antenna structure (24 m). To investigate this effect in detail, additional simulations were completed for the Teleost, with and without the antenna structures and the A-frame mast. Results are shown in Figs. 14 and 15.

Initially, the A-frame mast and the two antenna structures were completely removed from the developed model and Fig. 14 shows this simulation result; ie. the broadside null at 7 MHz has disappeared. This anti-resonant effect is further confirmed in Fig. 15 by sequentially removing one or both of the antenna structures and the A-frame mast. For instance, a difference of 15 dB is observed in Fig. 15 (d) with no stern antenna structures and A-frame. Similarly, the other model variations illustrate differences of ≤ 10 dB as shown in Figs. 15 (a) - (c). These results suggest that such secondary structures can act as resonant scatterers and that the RCS may be reduced due to certain vessel configurations. In future radar trials, it would be interesting to verify these RCS variations at the other frequencies, particularly the RCS null at 7 MHz.

C. Deviations Caused by Varied Weather Conditions

To investigate the effects of pitch and roll on RCS, the Teleost baseline model (Fig. 2) was advanced further. The varied rotations could be caused by ocean waves or unforeseen threats. Comparisons to the returns for the upright vessels

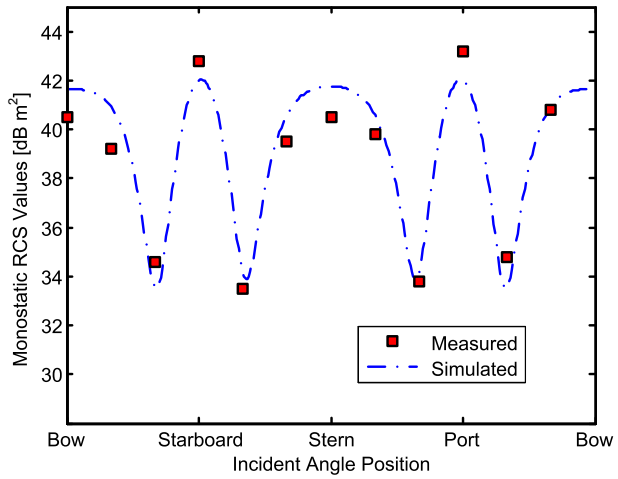

Fig. 9. Comparison of measured and simulated monostatic RCS return values for the Teleost vessel at 4.1 MHz.

could signify changes in the oceanic environment surrounding the ship. In general, knowledge of such variations from a baseline model could indicate if the vessel of interest is under some unwanted or unknown distress.

The effect of vessel pitch was first investigated by rotating the bow of the Teleost upwards by $5°$, $10°$ and $15°$. The differences between the monostatic RCS of the rotated model and the upright base model (i.e., normalization to the RCS in Fig. 11) are shown in Figs. 16-18; with increased bow movement additional variations are observed in the upright base model. For instance, mean variations of 0.70, 1.52 and 2.34 dB are observed for a $5°$, $10°$ and $15°$ bow rotation, respectively. In all cases, the RCS of the rotated ship could vary by at most 15 dB from the monostatic returns, thus suggesting a noticeable change in RCS. Similar results are expected for stern elevations.

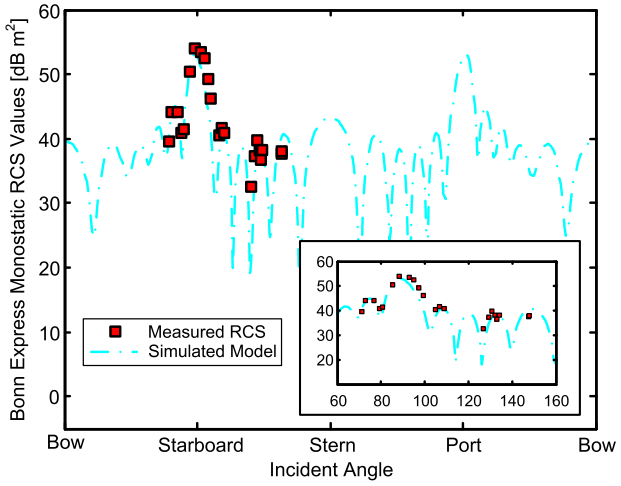

Fig. 10. Comparison of measured and simulated monostatic RCS return values for the Bonn Express freighter at 4.1 MHz.

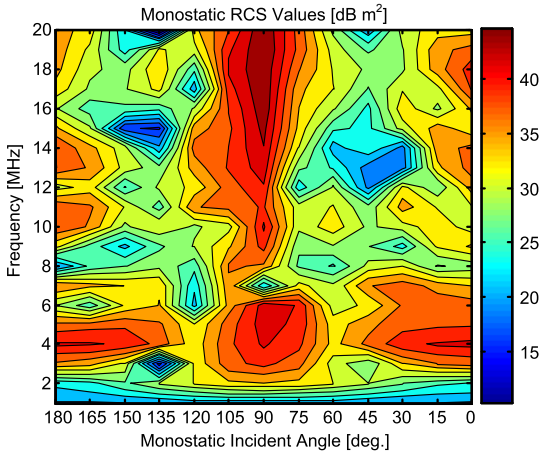

Fig. 11. Simulated monostatic RCS returns for the base model of the Teleost from 1 to 20 MHz.

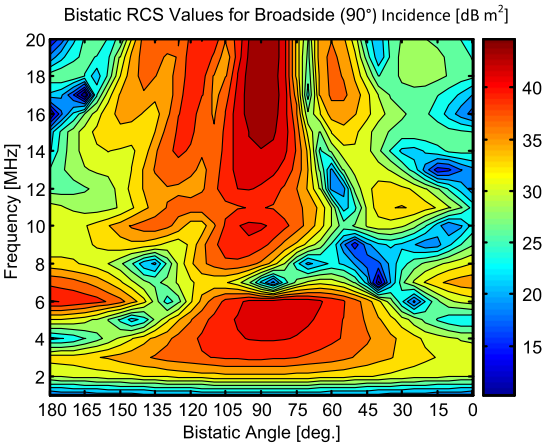

Fig. 12. Simulated bistatic RCS values with broadside incidence $(90°)$ for the Teleost model with antenna structures and A-frame mast (Fig. 4).

The effect of ship rolling in the port and starboard directions was also investigated. This was done by rotating the port side of the Teleost base model upwards by $5°$ and $10°$. Simulation results are shown in Figs. 19 and 20 with mean variations of 0.36 and 0.75 dB, respectively. In addition, the starboard side of the vessel was rotated by $5°$ as shown in Fig. 21 and a mean variation of 0.43 dB can be observed. It appears that these modeled alterations have a less significant effect on the monostatic RCS when compared to the vessel pitch rotations of Figs. 16-18.

D. Advancement of the Developed Models

In general, the Teleost and Bonn Express models have shown a very good agreement with measured results at 4.1 MHz. With additional RCS simulations a good agreement may be expected for higher frequencies of operation. For instance, slight deviations between measurements and the presented RCS simulations (monostatic and bistatic frequency analysis, Figs. 11-13, broadside null investigations, Figs. 14-15 and the model geometry variations due to varied weather

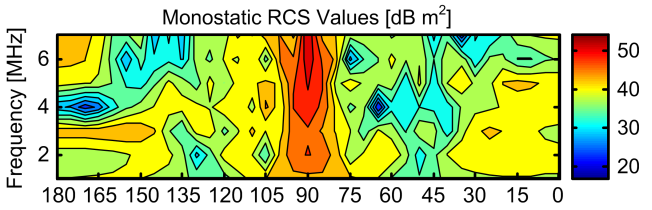

Fig. 13. Simulated monostatic RCS values for the Bonn Express freighter from 1 to 7 MHz.

conditions, Figs. 16-21) may occur due to the simplicity of the proposed FEKO models. At higher frequencies the inclusion of such details (multiple antennae, ship windows, varied cargo containers etc.) can escalate memory usage and computational complexity. Increased confidence is possible at high frequencies but at the cost of considerable simulation time, processing and computer resource requirements. At low frequencies such ship details are minor with respect to frequency and thus the presented models and simulation results may be valid for particular monostatic and bistatic returns.

III. Conclusions and Recommendations

This work has presented monostatic and bistatic RCS simulations of the Teleost and Bonn Express vessels. A very good agreement is achieved between measured and simulated values at 4.1 MHz, building confidence in the developed FEKO models. The effects of pitch, roll and freighter loading on RCS have also been investigated to account for practical situations in oceanic environments. Results show that the monostatic RCS of the Teleost could vary by at most 15 dB for a 10° roll or a 15° ship incline. The RCS simulations were also extended to other HFs. In the case of the Teleost, it was found that the simulated RCS has a broadside null at 7 MHz, likely due to a destructive resonant scattering of the antenna and A-frame

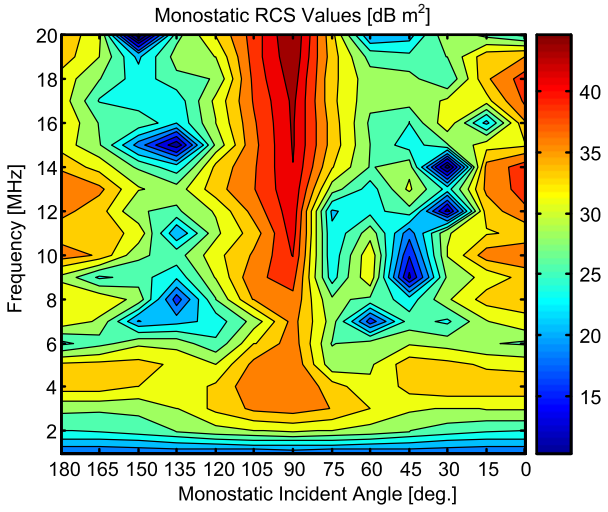

Fig. 14. Monostatic returns of the Teleost base model without the A-frame mast and antenna structures. The broadside null at 7 MHz is not observed.

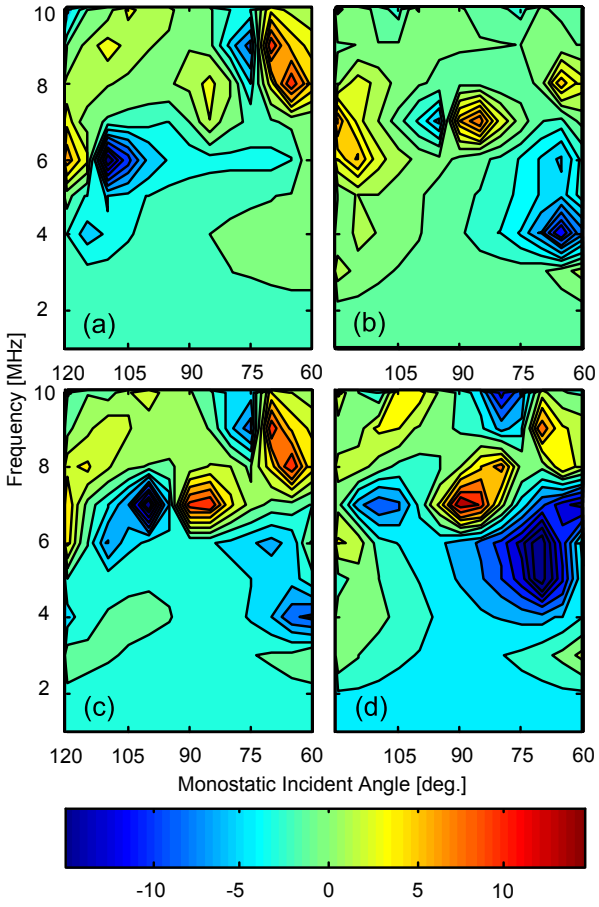

Fig. 15. Simulated monostatic returns using modified versions of the Teleost base model (a): without the bow antenna structure, (b): without the stern antenna structure, (c): without both antennae structures and just the A-frame and (d): without both antennae structures and without the modeled A-frame mast (same as Fig. 14). The difference from the nominal Telost simulation (Fig. 11) is shown in dB ($\sigma_{(a),(b),(c),(d)}/\sigma_{base}$). Results in (a) show that the bow antenna has a less significant effect on RCS, while in (d), an increase of 15 dB is observed by the absence of the antennae structures and A-frame.

structures on the ship. In future trials, it would be interesting to verify this with radar measurements.

References

[1] M. I. Skolnik, "An Emperical Formula for the Radar Cross Section of Ships at Grazing Incidence," *IEEE Transactions on Aerospace and Electronic Systems*, vol. 10, pp. 292, Mar. 1974.

[2] H. Leong and H. Wilson, "An Estimation and Verification of Vessel Radar Cross Section for High-Frequency Surface-Wave Radar," *IEEE Antennas and Propagation Magazine*, vol. 48, no. 2, pp. 11–16, Apr. 2006.

[3] R. Solomon, "An investigation in High Frequency Range Bistatic Radar Cross Section Values of Complex Structures" *Masters Thesis, Royal Military College of Canada*, Kingston, ON. CAN., Apr. 2008.

[4] D. E. Barrick, "First-Order Theory and Analysis of MF/HF/VHF Scatter from the Sea" *IEEE Transactions on Antennas and Propagation*, vol. 20, no. 1, pp. 2–10, Jan. 1972.

[5] M. I. Skolnik, "Radar Handbook," Second Edition, McGraw Hill, New York, 1990.

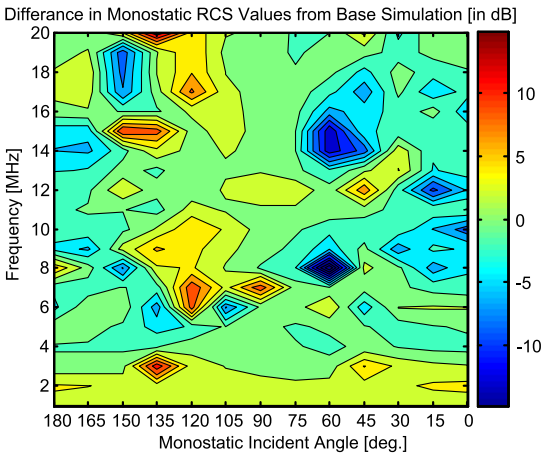

Fig. 16. Pitch Investigation: difference from the nominal Telost simulation (Fig. 11) with a 5° upward rotation of the bow ($\sigma_{5^\circ}/\sigma_{base}$ in dB).

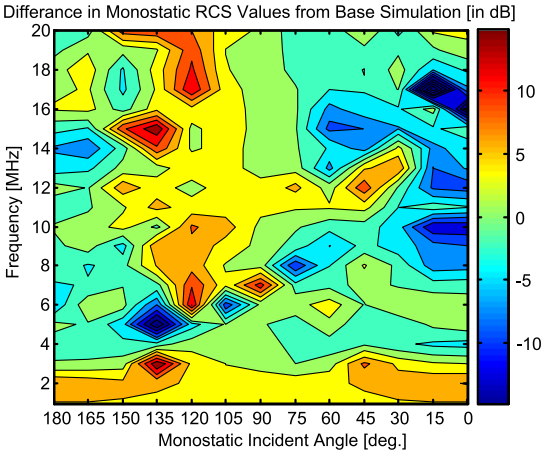

Fig. 17. Pitch Investigation: difference from the nominal Telost simulation (Fig. 11) with a 10° upward rotation of the bow ($\sigma_{10^\circ}/\sigma_{base}$ in dB).

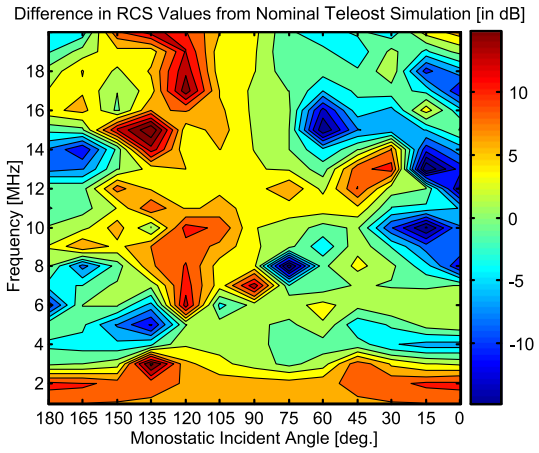

Fig. 18. Pitch Investigation: difference from the nominal Telost simulation (Fig. 11) with a 15° upward rotation of the bow ($\sigma_{15^\circ}/\sigma_{base}$ in dB).

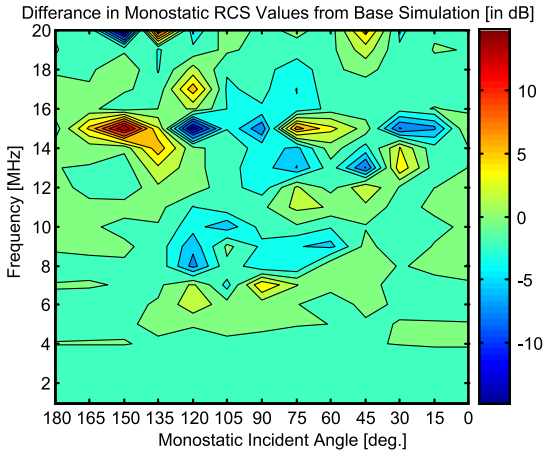

Fig. 19. Roll Investigation: difference from the nominal Telost simulation (Fig. 11) with a 5° upward rotation of the port ($\sigma_{5^\circ}/\sigma_{base}$ in dB).

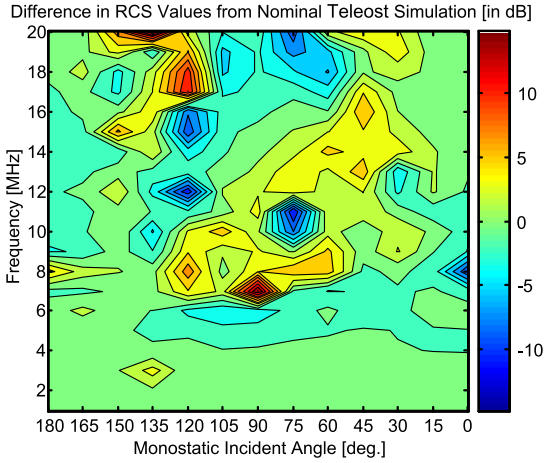

Fig. 20. Roll Investigation: difference from the nominal Telost simulation (Fig. 11) with a 10° upward rotation of the port ($\sigma_{10^\circ}/\sigma_{base}$ in dB).

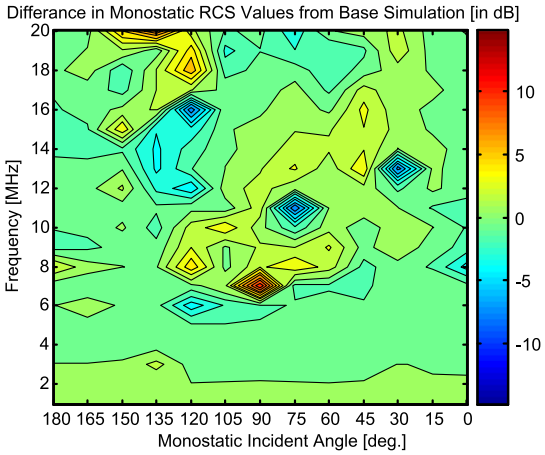

Fig. 21. Roll Investigation: difference from the nominal Telost simulation (Fig. 11) with a 5° upward starboard rotation ($\sigma_{5^\circ}/\sigma_{base}$ in dB).